

COB-2023- 2238

MEASUREMENT METHODOLOGIES FOR INVESTIGATING THE THERMAL BEHAVIOR OF A FERROUS MATRIX COMPOSITE REINFORCED BY CARBIDE OR NIOBIUM NITRIDE

Júlia Chisté Comunello

Isadora Schramm Deschamps

Federal University of Santa Catarina (UFSC), Campus Universitário Reitor João David Ferreira Lima, R. Delfino Conti, s/n - Trindade, Florianópolis - SC, 88040-900
julia.comunello@gmail.com, isadora.deschamps@labmat.ufsc.br

Isadora Hasselmann Machado

Federal University of Santa Catarina (UFSC), Campus Universitário Reitor João David Ferreira Lima, R. Delfino Conti, s/n - Trindade, Florianópolis - SC, 88040-900
isadora.h.m@labmat.ufsc.br

Aloísio Nelmo Klein

Federal University of Santa Catarina (UFSC), Campus Universitário Reitor João David Ferreira Lima, R. Delfino Conti, s/n - Trindade, Florianópolis - SC, 88040-900
a.n.klein@labmat.ufsc.br

Abstract. *This study investigates the coarsening behavior of niobium carbide (NbC) and nitride (NbN) reinforcements in an iron matrix composite. The production process is based on research carried out at the Materials Laboratory (Labmat) at UFSC and aimed at developing a cost-effective composite material that displays promising mechanical properties, owing to its submicrometric reinforcements. Thanks to the low solubility of niobium carbides in iron, such fine microstructure is expected to be retained even at higher temperatures. The aim of this study is to evaluate the coarsening sensitivity of such composite regarding different thermal cycles, in order to understand the extent to which operations, such as forging, hot pressing, cladding, welding, and cutting, could be made without compromising the composite's microstructure.*

Three heat treatment conditions were defined based on thermodynamic simulations using the Thermo-Calc® software: 1150°C for 10 hours 1500°C, for 1 hour; and 1150°C for 5 hours. Reinforcement analysis of the ferrous matrix was performed using image analysis and acid digestion followed by ZetaSizer® analysis. Coarsening was also simulated using PRISMA®. Mean reinforcement did not exceed 4 µm in any of the composites nor experimental measurements, which is lower than the 10 µm predicted by the simulations in the highest temperature condition. Moreover, the characterization methods and their overall reliability were thoroughly discussed considering the particularities of each technique.

Keywords: *MMC, Particulate Composite, Coarsening, Image and Experimental Analysis, Thermodynamic Properties.*

1. INTRODUCTION

The importance of Metallic Matrix Composites (MMC) materials resides in the possibility of joining high hardness, high wear resistance and high tenacity with competitive applicability to metallic alloys. The sum of these factors along with high structural efficiency, excellent wear resistance and attractive thermal and electrical characteristics, are advantages that expanded and perpetuated its application for the automotive, aerospace, land transport and infrastructure industries, among others (Miracle, 2005). Aluminum and titanium matrices reinforced by carbides and nitrides are frequently employed in MMCs, especially where a low density is required in their final applications. Ferrous matrix composites, in turn, do not have a significant presence in the current market, since high-alloy steels already contain up to 20% of carbides in their volumetric concentration; however, the carbides and nitrides present in high-alloy steels are soluble and have significantly coarsening rates in higher temperatures.

In the case of an MMC, it is possible to achieve a higher volumetric concentration since the reinforcement doesn't need to be dissolved in the matrix. This advantage can lead to promising increases in wear resistance and hardness, and the use of carbides and nitrides is studied for this purpose. Prioritizing elements with low free energy make these components even more stable; this is the case for carbides and nitrides of elements such as niobium, titanium and vanadium. Moreover, a ferrous matrix composite can bring an optimal relationship between cost and properties, along

with potentially being subjected to additional thermal treatments depending on the target properties (Avila, 2020; Guan et al., 2018).

In that sense, our research group has observed through thermodynamic simulations that both NbC (niobium carbide) and NbN (niobium nitride) have great thermal stability (up to 1500 °C), high hardness and low interface energies – NbN approximately at 0.86 J/m², and NbC from 0.1 J/m² reaching up to 1 J/m² - in the case of a coherent or semi-coherent interface acquired with ferrite or austenite. It is thus expected that such carbides or nitrides would present a low coalescence rate (Avila, 2020).

Coarsening - that is, particle growth through mass reallocation - is influenced by high temperatures and the duration period and cooling rates of such; hence, it is a characteristic that must be investigated in cases that require a hard and resistant material (Chiaverini, 1986), as excessive coarsening has direct consequences on the decrease in strength and increase in ductility in the final mechanical properties of the material.

Both the solubility and diffusivity of an element in a given phase increase with temperature, so the higher the temperature, more susceptible to coalescence is a composite. That being so, the phenomena of size increase in reinforcement particles at high temperatures vary according to the composition, as well as processing and application temperatures. Therefore, the purpose of this work lies in the modeling and characterization of particle growth caused by the coalescence of reinforcing particles of a ferrous matrix composite reinforced by niobium nitrides and carbides, so as to map limits and potentials in the applicability and processing operations for these composites.

2. METHODOLOGY

2.1 Thermo-Calc® simulations for the assessment of heat treatments

In this initial step, the thermodynamic simulation software Thermo-Calc® was exploited as a guidance tool before the experimental process, providing insight into the establishment of the heat treatment conditions. Using the *Thermo-Calc® Property Diagram* template, the elements and their respective percentages by mass, species and phase constitution were used to simulate stable phases of the Fe-NbC and Fe-NbN systems as a function of temperature. With this, it was possible to delimit the conditions of heat treatments (C1, C2 and C3) that could help further understand the coalescing of reinforcements.

Simulation of the coarsening of the grains was also performed on the selected heat treatments conditions, using the complementary precipitation module (TC-PRISMA®), the “Steels and Fe-alloys (TCFE11, MOVFE6)” package, and the “TCFE11:steels/Fe-Allows v1.0” and “MOBFE6:Steels/Fe-Allows Mobility v6.0” databases. The “Nucleation Sites” (nucleation regions) were set as 0 /m⁻³s, and the interfacial energy values were chosen according to the previously mentioned literature, with different coefficients for NbC (0.1 J/m² and 0.5 J/m²) since the results found were inconclusive. Properties related to strain (“Transformation Strain”), growth rate model (“Growth Rate model”), morphology (“Morphology”) and phase boundary mobility (“Phase boundary Mobility”) were set in default. Since the “Preexisting Size Distribution” parameter supports the addition of a table with radius size vs. numerical density, it is possible to add the results regarding the sizes of the reinforcements with the composites already precipitated and still without subsequent thermal processes. Thus, the tables for both reinforcements were made with data from the acid digestion method. For each of the reinforcements (NbC and NbN), two simulations were performed: 1150°C with 10h of holding time and 1500°C with 1h holding time.

2.2 Heat treatments

Using the result of the property diagrams from Figures 1 and 2, heat treatments were stipulated to encourage different degrees of coalescence of the NbN and NbC reinforcements.

Table 1. Heat Treatment conditions determined by the Thermo-Calc® simulations.

Heat Treatment Conditions	Temperature (°C)	Hold (h)	Atm	Equipment
C0 ⁽¹⁾	as received ⁽¹⁾	as received ⁽¹⁾	as received ⁽¹⁾	as received ⁽¹⁾
C1	1150	10	Ar	Tubular Furnace, model FT1200/H-3z
C2	1500	1	Ar	Furnace, model FT-1700/H/GAS
C3	1150	5	Ar	Tubular Furnace, model FT1200/H-3z

⁽¹⁾ Fe-NbN and Fe-NbC composites in the received original state, already precipitated but without subsequent thermal processes for coarsening to serve as a comparison agent.

2.3 Particle Size Analysis Methods

For the reinforcement size measurements of the Fe-NbN and Fe-NbC composite samples after the thermal treatments, two methods were used; the acid digestion of the reinforcements followed by its valuation on a ZetaSizer®, and image analysis in Fiji® through the results obtained by SEM (Scanning Electron Microscopy).

2.3.1. Acid Digestion

A solution with 30% HCl was used in the samples to dissolve the ferrous matrix, leaving only the ceramic reinforcements (nitrides/carbides) in solid form. To facilitate the process, the reactions were kept on a magnetic stirrer. Using the KASVI® 300-4000RPM benchtop centrifuge, the separation process between reinforcement and acid was carried out in stages to gradually decrease the acid concentration, by settling the suspended particles, removing acid and diluting it by adding distilled water. This cycle was repeated until samples reached a pH near 6. The final solution with carbide or nitride particles that were measured using a ZetaSizer®.

2.3.2. Image Analysis

The average particle size was also determined using the Fiji® software for image analysis and manipulation. For each condition carried out in the laboratory (conditions 1 to 3) in samples of carbide and nitride reinforcements, 10 SEM-BSE photos were used, in magnitudes of 10-20kx.

A methodology was implemented for establishing the area of the reinforcement particles. After the proper scale and resolution adjustments, modifications using the “*Non-Local Means Denoising*” (plugin NLM), “*Unsharp Mask*”, “*Median*” and “*Contrast*” filters were used to eliminate noise with the preservation of particle boundaries, while favoring the contrast of the reinforcement particles. Next, the “*Threshold*” and “*Watershed*” filters were used, followed by an erosion of the grain boundaries and removal of the edges to disregard non-integer particles. The final segmentation was performed by applying the MorphoLibJ plugin, whose “*Morphological Segmentation*” functionality enables the count of particles and their respective areas. After this, the total area averages were converted into average particle size radius for each sample and condition, enabling the data and comparisons performed.

3. RESULTS AND DISCUSSION

3.1 Thermal treatments and particle growth Thermo-Calc® simulations

Properties diagrams were simulated for the composite using the two types of reinforcements, NbN and NbC. The results are as shown below, in Figures 1 and 2.

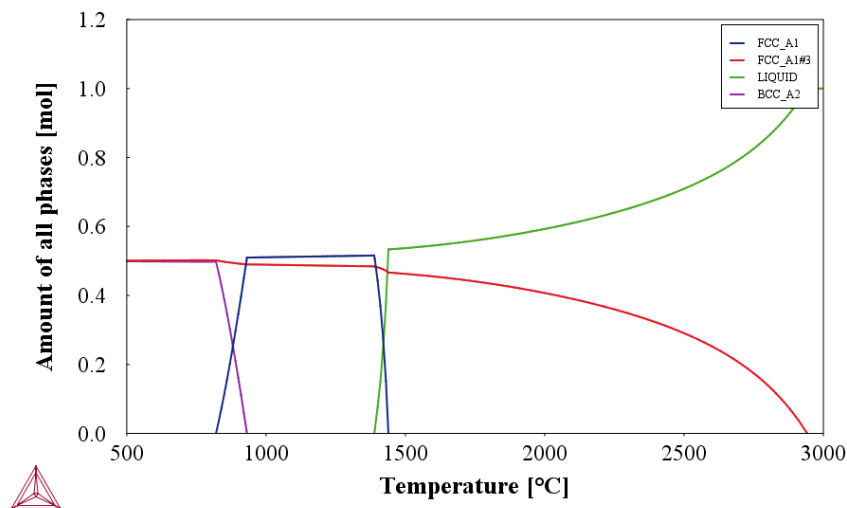


Figure 1. Properties diagram of the composite with carbide (NbC) reinforcement, in Thermo-Calc®.

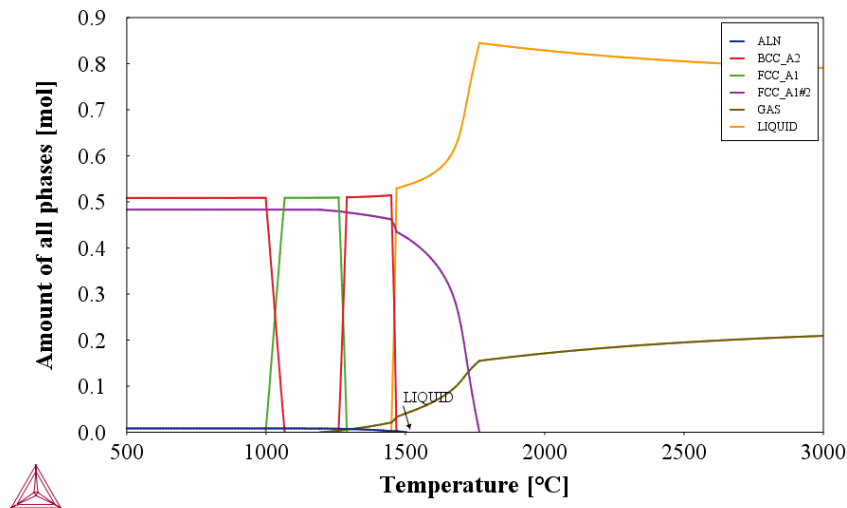


Figure 2. Properties diagram of the composite with nitride (NbN) reinforcement, in Thermo-Calc®.

As expected, the carbide-reinforced composite (FCC_A1#3 of Figure 1) shows a more significant coarsening after the reinforcement melts, as is also the case of the nitride-reinforced composite (FCC_A1#2 of Figure 2), which portrays the niobium progressively dissolving as the amount of N₂ increases. In other words, in both cases there is a noticeable molar volume loss of the reinforcement phases while the amount of liquid increases, indicating the reinforcement dissolution. In quantitative terms, this material starts melting at approximately 1440° C when the reinforcements are carbides, and 1490° C when they are nitrides. According to these definitions, the conditions of 1150° C in 10h and 5h and 1500° C in 1h were then defined for the next simulations, to set the behavior of the reinforcements right before and after their theoretical melting point.

For the particle growth simulations in the TC-PRISMA®, the output generated were plots of mean radius size (µm) vs. duration (h) t, defined as the “expected” mean results for the size of reinforcements due to the coarsening of the experimental samples. The simulations were made with both reinforcements (NbN and NbC) in all heat cycles considered.

The results assembled in Figure 3 indicated that condition C2 (1500° C in 1h, Figure 3.b) showed coarsening of both reinforcements. A significant growth compared to C0 is observed among all tested reinforcements (NbC (0.5 J/m²), NbC (0.1 J/m²) and NbN (0.86 J/m²)). For the simulation regarding the condition of 1150° C during 5h/10h (Figure 3.a), it was verified that a 5h hold on both reinforcements wasn’t sufficient for inducing a coarsening effect. As for a duration of 10h, there is a low coarsening (if compared to the absolute values of the previous simulation) for NbN (0.86 J/m²), while NbC (0.5 J/m²) remains unaffected by the property. NbC (0.1 J/m²) was not investigated in this case, since a lower interface energy would bring a smaller growth and, therefore, the same result.

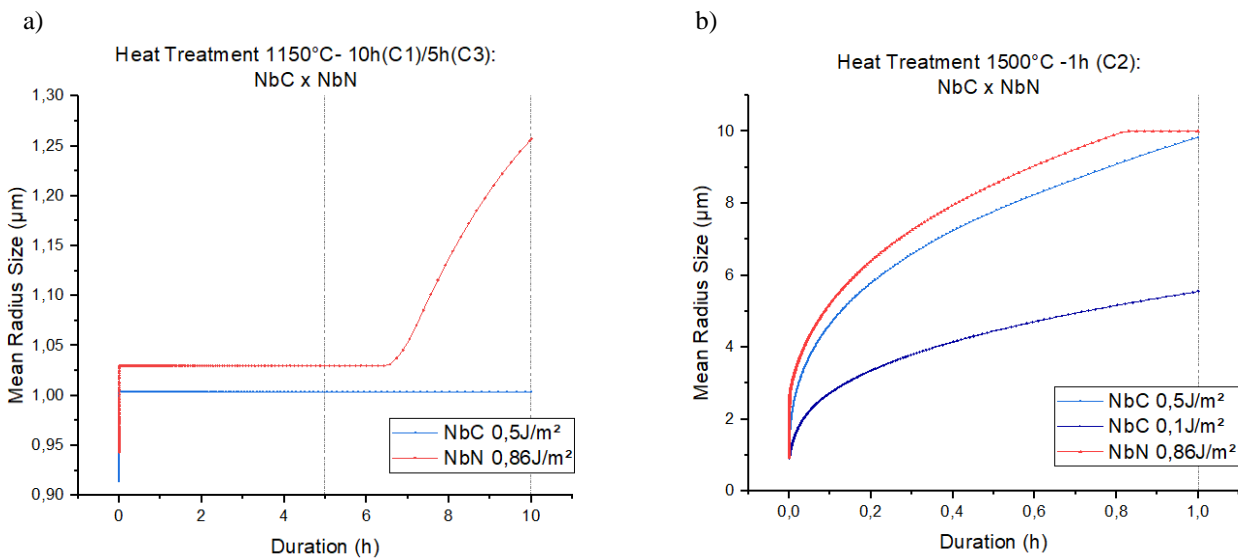


Figure 3. a) TC-PRISMA® coarsening simulation results of the NbN and NbC reinforcements at 1150°C for 10h/5h (C1/C3); b) TC-PRISMA® coarsening simulation results of the NbN and NbC reinforcements at 1500°C for 1h (C2).

3.2 Acid Digestion

The particle size obtained through acid digestion and measured by ZetaSizer® generated distribution values of the average size of the particle radius (μm) for the carbide and nitride reinforcements, given three different counts that were performed for each sample, “Record 1”, “Record 2” and “Record 3”. They were subsequently simplified to the mean radius size (μm) between the reinforcements (NbN and NbC) under conditions 0, 1, 2 and 3 to the values in Table 2.

3.3 Image Analysis

Examples of the image processing according to the Fiji® software and overall methodology are shown in Figure 4.

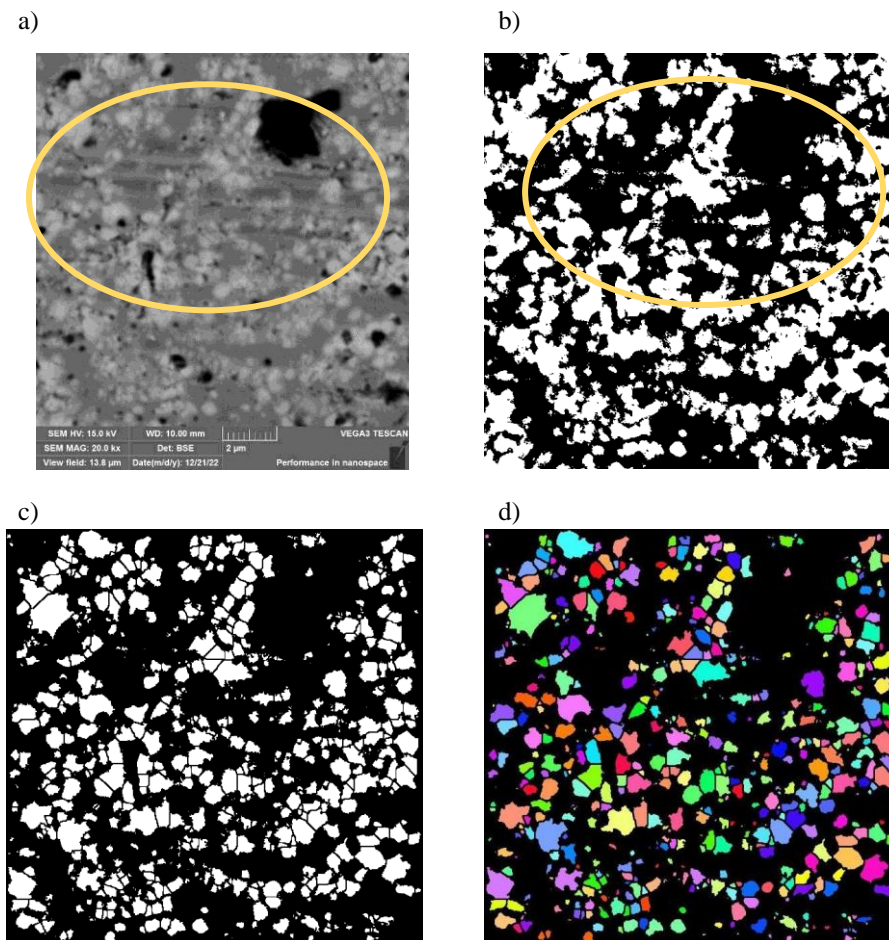


Figure 4. a) SEM Image of the carbide reinforcements in mag. 20kx, in condition 0; b) Fiji® treatment up to the “Watershed” filter; c) Fiji® treatment after cleaning, erosion and removal of edges; d) Final image in Fiji® after the “Morphological Segmentation” filter.

Due to the noise occurrence from the sample preparation process (as exemplified in Figure 4.a and 4.b), many “false particles” were observed, calculated by the software as part of the reinforcement size distribution. To reduce this disturbance, particle sizes were taken below $1 \mu\text{m}$ for the samples related to C1 and $0.2 \mu\text{m}$ in the rest of the heat treatments (C0, C2 and C3).

Another adjustment made was due to the randomness of the cut section of the samples performed for SEM analysis. This means that the radius observed (R_i) by the SEM image didn’t necessarily correspond to the real radius of the particle (R_p), as they could have been cut before or after the maximum radius size of the reinforcement – a concept schematized in Figure 5. Thus, a probabilistic adjustment was necessary to account for this uncertainty in the measured radii.

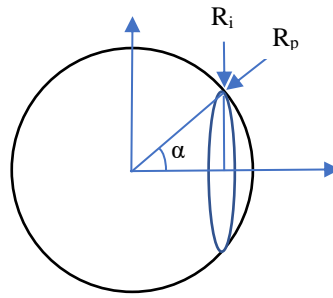


Figure 5. Scheme of a reinforcement particle on the relation between R_i (observed value of reinforcement radius) and R_p (true value of reinforcement radius).

Approaching the reinforcements in a spherical shape, it can be stated that:

$$R_i = R_p \sin \alpha \quad (1)$$

For the data statistical treatment, it is considered that the expected value for the true reinforcement radius (R_p) is composed of the radii of the sections and the angle (α) of the cut:

$$E[R_i] = E[R_p \sin \alpha] \quad (2)$$

The variables true radius (R_p) and angle (α) are independent. Thus, the expected value of the product of these two variables is the product of the expected values for each one:

$$E[R_i] = E[R_p]E[\sin \alpha] \quad (3)$$

The random sine wave is in the α ($0, \pi/2$) domain and its expected value is found by the integral:

$$E[\sin \alpha] = \int_0^{\pi/2} x f_X(x) dx \quad (4)$$

Where $f_X(x)$ is the probability density function for the domain. The angle has a uniform distribution in the domain, which results in the following probability density function:

$$f_X(x) = \frac{2}{\pi} \frac{1}{\sqrt{1-x^2}} \quad (5)$$

By introducing Eq. 5 into Eq. 4, we arrive at:

$$E[\sin \alpha] = \frac{2}{\pi} \quad (6)$$

Returning to Eq. 2, the expected value of the true reinforcement radius (R_p) needs to be adjusted by the expected value of the sine of the random angle (α), which becomes:

$$E[R_p] = \frac{\pi}{2} E[R_i] \quad (7)$$

Finally, Eq. 7 becomes the outcome of the necessary adjustment, resulting in a 57% increase in the relative ray size values and in the overall average per sample. This adaptation is already incorporated in the results of Table 2.

3.4 Methodologies comparisons

The results obtained in the form of mean radius sizes (μm) off the Thermo-Calc® simulations, acid digestion results in ZetaSizer® and image analysis through the Fiji® software using the four heat cycles conditions can be seen in Table 2 and in Figure 6.

Table 2. Means radius size (μm) distributions of NbN and NbC particles under Conditions 0, 1, 2 and 3 of the Thermo-
Calc® simulations, acid digestion and image analysis results.

Mean radius size							
Condition Heat Cycle	Type of Reinforcements	T-Calc® results (μm)	% (Relative to C0)	Zetasizer® results (μm)	% (Relative to C0)	Fiji® results (μm)	% (Relative to C0)
C0	NbC	0,913	-	0,877	-	0,447	-
	NbN	0,943	-	0,683	-	0,447 ⁽³⁾	-
C1	NbC	1,003	9,8%	1,295	47,3%	0,491	9,9%
	NbN	1,257	33,3%	1,340	96,2%	0,446	0,2% ⁽³⁾
C2	NbC	7,806 ⁽¹⁾	754% ⁽¹⁾	2,720	210%	3,760	741%
	NbN	9,057	960%	3,220	371%	2,086	366% ⁽³⁾
C3	NbC	1,004	9,8%	2,440	178%	0,456	2%
	NbN	1,029	9,2%	0,016 ⁽²⁾	-97,5% ⁽²⁾	0,431	-0,3% ⁽³⁾

⁽¹⁾ Mean between different values of NbC interface energies.

⁽²⁾ Value at which it is believed to account for defects in the acid digestion process.

⁽³⁾ Data of NbN / C0 were not obtained since the sample in powder form could not be observed in the SEM. They were considered equivalent to carbide to validate subsequent comparisons, as they showed great similarity in acid digestion and simulations.

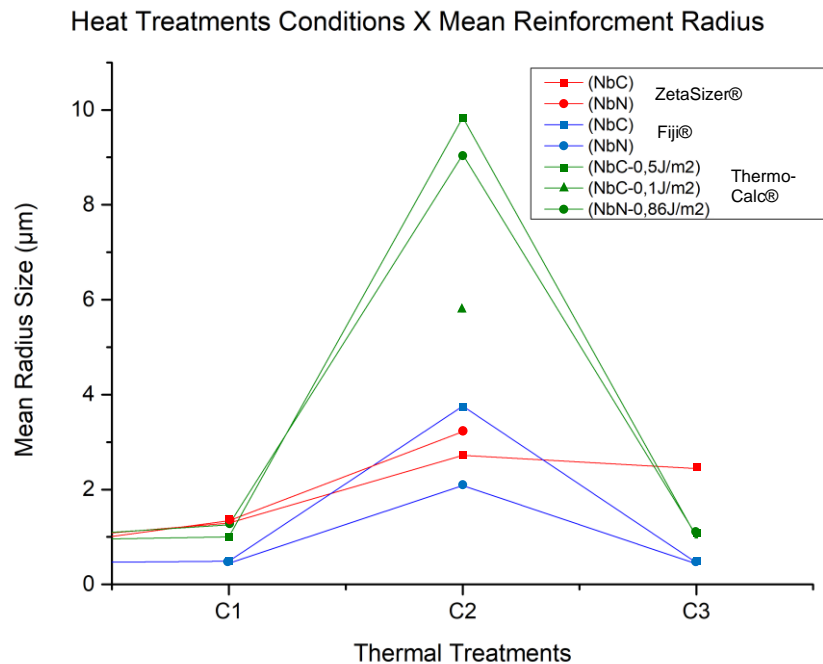


Figure 6. Graph containing all methodologies absolute values of NbN and NbC reinforcements in the C0,1,2 and 3 conditions.

By plotting the observed data (Figure 6), it is noticeable that there was a common trend among the results obtained by all methods. The mean particle sizes tended to remain similar to their initial conditions, with only a significant increase in the treatment at 1500°C (C2), when the samples were treated with a value above their melting temperature. The observed coarsening was, however, smaller than expected both through the characterization by acid digestion and through image analysis, as seen for the absolute radius values that remained below 4 μm while the simulations estimated particles growing up to 10 μm as stated in Figure 3.b.

From both visual representations, comparisons can be made on the results of the 3 coalescence evaluation methods. The C0 and C1 samples were the most quantitative similar among all methods, especially between the acid digestion and the simulation methods, with values of 0.88 μm for 0.91 μm in NbC/C0, 0.68 for 0.94 in NbN/C0, 1.29 μm

for 1 μm in NbC/C1 and 1.34 μm for 1.25 μm in NbN/C1, respectively. The Zetasizer® results of C0 and C1 intermediates the Thermo-Calc® and Fiji® values, with a slight increase of 47% in C1 in relation to C0 for carbides and 96% for nitrides. This makes sense considering that the C0 values obtained in the ZetaSizer® were used in the Thermo-Calc® calculations.

However, the absolute values similarities start to diverge considerably for the values of C2 and C3. In C2, the data acquired through Zetasizer® and Fiji® are closer, with 2.72 μm and 3.7 μm for NbC and 3.22 μm and 2.08 μm for NbN, respectively. On the other hand, despite the Fiji® results registering significantly smaller values of average particle size, there is a greater similarity in reinforcement growth when compared to the simulations. The results for NbC/C1 indicated 9.9% and 9.8%, NbC/C2 741% and 754% and NbC/C3 2% and 9.8% increase in comparison to their reinforcements in C0 for the analysis of image and simulation, respectively. Considering micrometric quantities, the similarity in growth percentage is significant.

The choice for the property diagrams, the particle growth simulations and two reinforcement size measurement systems were made in an attempt to obtain a more complete evaluation of the property of interest, in addition to clarifying its specificities and ways in which these methods can be improved. Regarding the simulation calculations, certain variables were not optimized due to the lack of a complete understanding of the studied composites, such as the interface energy itself and the maintained standard variables; there are also limitations of the software model itself, which may not cover all aspects of this particular composite. At the same time, as it entails a reproducible numerical method it is inferred that all variables will have the same influence during all simulations and therefore less processing abnormalities, as it possibly could be in an experimental method. In terms of comparison between the same sample in different conditions, this is valuable although the absolute size can possibly not portray accurate values.

In the case of the analysis model made through acid digestion, this technique is extremely interesting since it results in loose particles available for analysis only related to the reinforcement of interest. Among the problems found, there was external contamination, such as alumina from the grinding processes, possible erosion of the glass beaker due to the long periods of agitation time of very hard reinforcements, and incomplete digestion of the matrix - these are circumstances believed to have caused unusual results of the NbN from C3 shown in Table 2. In addition, the process can become time-consuming depending on the number of samples and equipment available. In terms of the robustness of results obtained, the sampling count was extremely low in the Zetasizer® equipment; acid digestion revealed total counts in the hundreds, while image analysis counted thousands of reinforcements. This low sampling influenced the mean value, becoming more susceptible to the aforementioned problems. The greatest advantage was the measurement of the actual radius of the precipitates with fewer experimental issues, observed through the individual results of the C0 and C1 samples.

For measurements related to image analysis performed by Fiji®, the methodology itself is extensively supported by traditional reinforcement size studies and therefore evokes a greater sense of reliability – which does not mean that there are no disadvantages when considering the particularities of this design, as the need for adjustments due to sample quality and the probabilistic radius adaptation were proof of it. These adjustments are the result of the biggest dilemma of this process, which resides in the fact that the analysis is completely dependent on the circumstances of the image performed in SEM; the inaccuracies between the reinforcement contours made visual considerations difficult, and consequently the division of areas and size. However, the actions taken made the average result more faithful in terms of comparison. Analogously to the Thermo-Calc® method, the reproducibility of a computational model is translated into robust comparative values, which was indicated by some similarities with the Thermo-Calc percentage grown trends even when considering divergent absolute values.

4. CONCLUSION

It was possible to verify that despite some differences between values and growth rates, the three attempted methods followed the same trend of increase and decrease between the tested conditions, with more expressive values of growth in the size of the precipitates in C2, whose temperature of threshold was higher than the melting temperature of the NbN and NbC reinforcements. In addition to corresponding with the progression of the simulations, the experimental results indicated that this coarsening is smaller than expected, with an average particle size below 4 μm for both NbN and NbC, while simulated results pointed to values greater than twice these data, above 9 μm in both cases. This indicates that both reinforcements are less sensible to coarsening and, therefore, to the degradation of their mechanical properties.

Considering the particularities of the methodologies developed, it was noticed that the simulated products were dependent on values whose concepts were not clearly defined, inhibiting more exact projections. That could be solved with other Thermo-Calc® packages and mobility databases, as well as more tests isolating these variables.

From the data obtained from acid digestion, as an experimental process less applied to the subject some procedural difficulties including low sampling and contamination impaired the view of the actual size of some precipitate's samples. This method, however, brought solid absolute values of reinforcements that showed fewer procedural defects.

On the other hand, although the analyses carried out in Fiji® provided greater precision in the method itself they were completely dependent on the SEM image quality, which, for the magnitudes and morphologies scope of this project specifically, added difficulties to the methodology.

Therefore, this body of work has critically evaluated the methods of coarsening determination and indicated the versatility that this specific process and composition has in terms of post-processing. This work has also mapped the microstructural evolution in the face of temperature-intensive processes, such as hot isostatic pressing (HIP), direct additive manufacturing with melting of the matrix, welding, etc.

5. ACKNOWLEDGEMENTS

The authors want to acknowledge Fundação de Ensino e Engenharia de Santa Catarina (FEESC), Instituto Hercílio Randon (IHR), and CNPq (National Council for Scientific and Technological Development) for the financial support.

6. REFERENCES

- Avila, D. Desenvolvimento de compósito de matriz ferrosa reforçado por carbeto de nióbio formado in situ durante a sinterização. . [S.l: s.n.], 2020.
- Chiaverini, V. Aços e Ferros Fundidos. 1986.
- Guan, D. et al. Tribological and corrosion properties of PM 316L matrix composites reinforced by in situ polymer-derived ceramics. *Vacuum*, v. 148, p. 319–326, 1 fev. 2018.
- Miracle, D. B. Metal matrix composites - From science to technological significance. *Composites Science and Technology*, v. 65, n. 15- 16 SPEC. ISS., p. 2526–2540, dez. 2005.

7. RESPONSIBILITY NOTICE

The authors are the only ones responsible for the printed material included in this paper.